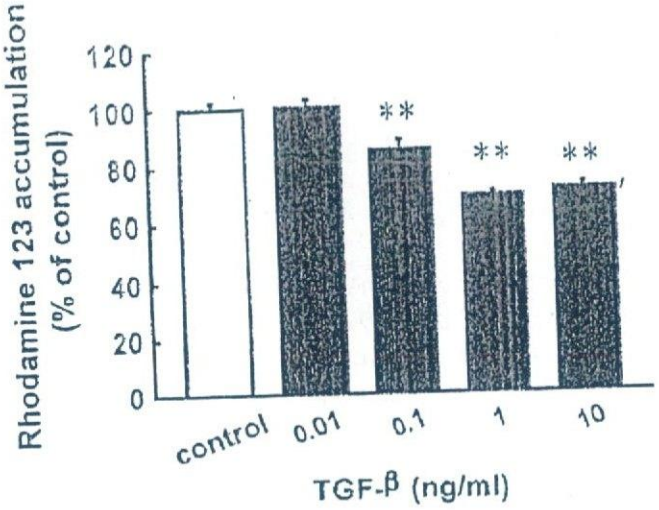

Fig. 2. Changes in the cellular accmulation of rhodamine 123 in MBEC4 cells after exposure to various concentrations of TGF-β1 for 12 h. The cellular accumulation of rhodamine 123 in MBEC4 cells for the control was 1.65 ± 0.05 nmol/mg protein. Data are expressed as percentages of control. Values are shown as means ± SEM (n = 4–10). $^{**}P < 0.01$; significant difference from control.

of control after a 12-h exposure to TGF-β1 at concentrations ranging from 0.1 to 10 ng/mL.

DISCUSSION

The permeability of Na-F and EBA through the MBEC4 monolayer was reduced by TGF-β1 and the accumulation of rhodamine 123 into MBEC4 cells was significantly decreased by TGF-β1. This action of TGF-β1 appeared within 3 h after treatment. These findings suggest that TGF-β1 supports the maintenance of BBB functions by integrating tight junctions and activating a P-gp-related transport system. The epithelial and endothelial barrier of paracellular permeability through tight junctions is known to be regulated by various signaling molecules including protein kinase C. Activation of protein kinase C is involved in the TGF-β signaling pathway (Halstead *et al.*, 1995), leading to a decrease in the permeability of brain microvascular endothelial cells (Raub, 1996). TGF-β-enhanced BBB functions in the early stage may be interpreted as occurring due to protein kinase C activation. TGF-β mediates multifunctional effects by eliciting transcriptional responses in many target genes. TGF-β1 increased *mdr1* gene expression via a protein kinase C-related signal transduction pathway (Utsunomiya *et al.*, 1997). The other TGF-β signaling cascades from membrane to nucleus could be involved in an enhancement of BBB functions, such as mitogen-activated protein kinase (Hartsough and Mulder, 1995) and a receptor serine/threonine kinase pathway (Wrana *et al.*, 1994). It is, therefore,

conceivable that TGF-β facilitates the barrier function and P-gp functional activity of brain endothelial cells by increasing the expression of tight junction-associated proteins (such as occludin and claudins) and P-gp. Endothelial cells, when co-cultured with pericytes, produced an activated form of TGF-β (Antonelli-Olridge *et al.*, 1989) and elevated transendothelial electrical resistance (Dente *et al.*, 2001), suggesting that TGF-β production by pericytes is significant for maintaining the integrity of the BBB.

In the present study, we demonstrated that TGF-β1 lowered endothelial permeability and increased the functional activity of the P-gp efflux pump in MBEC4 cells. These findings suggest that cellular constituents producing TGF-β in the brain may keep the BBB functioning.

ACKNOWLEDGMENTS

This work was supported in part by a Grant-in-Aid for Scientific Research ((B)(2) 14370789) from the Ministry of Education, Culture, Sports, Science and Technology (MEXT), Japan, and by funds (No. 031001) from the Central Research Institute of Fukuoka University.

REFERENCES

Antonelli-Orlidge, A., Saunders, K. B., Smith, S. R., and D'Amore, P. A. (1989). An activated form of transforming growth factor β is produced by cocultures of endothelial cells and pericytes. *Proc. Natl. Acad. Sci. U.S.A.* **88**:4544–4548.

Bradford, M. M. (1976). A rapid and sensitive method for the quantitation of microgram quantities of protein utilizing the principle of protein-dye binding. *Anal. Biochem.* **72**:248–254.

Dehouck, M.-P., Jolliet-Riant, P., Brée, F., Fruchart, J.-C., Cecchelli, R., and Tillement, J.-P. (1992). Drug transfer across the blood–brain barrier: Correlation between in vitro and in vivo models. *J. Neurochem.* **58**:1790–1797.

Deli, M. A., Descamps, L., Dehouck, M.-P., Cecchelli, R., Joó, F., Ábrahám, C. S., and Torpier, G. (1995). Exposure of tumor necrosis factor-α to luminal membrane of bovine brain capillary endothelial cells cocultured with astrocytes induces a delayed increase of permeability and cytoplasmic stress fiber formation of actin. *J. Neurosci. Res.* **41**:717–726.

Dente, C. J., Steffes, C. P., Speyer, C., and Tyburski, J. G. (2001). Pericytes augment the capillary barrier in in vitro cocultures. *J. Surg. Res.* **97**:85–91.

Flanders, K. C., Ren, R. F., and Lippa, C. P. (1998). Transforming growth factor-βs in neurodegenerative disease. *Prog. Neurobiol.* **54**:71–85.

Fontaine, M., Elmquist, W. F., and Miller, D. W. (1996). Use of rhodamine 123 to examine the functional activity of P-glycoprotein in primary cultured brain microvessel endothelial cell monolayers. *Life Sci.* **59**:1521–1531.

Halstead, J., Kemp, K., and Ignotz, R. A. (1995). Evidence for involvement of phosphatidylcholine-phospholipase C and protein kinase C in transforming growth factor-β signaling. *J. Biol. Chem.* **270**:13600–13603.

Hartsough, M. T., and Mulder, K. M. (1995). Transforming growth factor β activation of $p44^{mapk}$ in proliferating cultures of epithelial cells. *J. Biol. Chem.* **270**:7117–24.

Orlidge, A., and D'Amore, P. A. (1987). Inhibition of capillary endothelial cell growth by pericytes and smooth muscle cells. *J. Cell Biol.* **105**:1455–1462.

Ramsauer, M., Krause, D., and Dermietzel, R. (2002). Angiogenesis of the blood-brain barrier in vitro and the function of cerebral pericytes. *FASEB J.* **16**:1274–1276.

Raub, T. J. (1996). Signal transduction and glial cell modulation of cultured brain microvessel endothelial cell tight junctions. *Am. J. Physiol.* **271**:C495–C503.

Rubin, L. L., and Staddon, J. M. (1999). The cell biology of the blood–brain barrier. *Annu. Rev. Neurosci.* 22:11–28.

Sato, Y., and Rifkin, D. B. (1989). Inhibition of endothelial cell movement by pericytes and smooth muscle cells: activation of a latent transforming growth factor-β1-like molecular by plasmin during co-culture. *J. Cell Biol.* **109**:309–315.

Tatsuta, T., Naito, M., Mikami, K., and Tsuruo, T. (1994). Enhanced expression by the brain matrix of P-glycoprotein in brain capillary endothelial cells. *Cell Growth Differ.* **5**:1145–1152.

Tatsuta, T., Naito, M., Oh-hara, T., Sugawara, I., and Tsuruo, T. (1992). Functional involvement of P-glycoprotein in blood-brain barrier. *J. Biol. Chem.* **267**:20383–20391.

Utsunomiya, Y., Hasegawa, H., Yanagisawa, K., and Fujita, S. (1997). Enhancement of *mdr1* gene expression by transforming growth factor-β1 in the new adriamycin-resistant human leukemia cell line ME-F_2/ADM. *Leukemia* **11**:894–895.

Wang, W., Merrill, M. J., and Borchardt, R. T. (1996). Vascular endothelial growth factor affects permeability of brain microvessel endothelial cells in vitro. *Am. J. Physiol.* **271**:C1973–C1980.

Wrana, J. L., Attisano, L., Wieser, R., Ventura, F., and Massagué, J. (1994). Mechanism of activation of the TGF-β receptor. *Nature* **370**:341–347.

Cellular and Molecular Neurobiology, Vol. 24, No. 2, April 2004 (© 2004)

Uptake and Efflux of Quinacrine, a Candidate for the Treatment of Prion Diseases, at the Blood-Brain Barrier

Shinya Dohgu,[1,2] Atsushi Yamauchi,[2] Fuyuko Takata,[2] Yasufumi Sawada,[1] Shun Higuchi,[1] Mikihiko Naito,[3] Takashi Tsuruo,[3] Susumu Shirabe,[4] Masami Niwa,[4] Shigeru Katamine,[4] and Yasufumi Kataoka[2,5]

Received April 7, 2003; accepted May 22, 2003

SUMMARY

1. A clinical trial of quinacrine in patients with Creutzfeldt–Jakob disease is now in progress. The permeability of drugs through the blood–brain barrier (BBB) is a determinant of their therapeutic efficacy for prion diseases. The mechanism of quinacrine transport across the BBB was investigated using mouse brain endothelial cells (MBEC4).

2. The permeability of quinacrine through MBEC4 cells was lower than that of sodium fluorescein, a BBB-impermeable marker. The basolateral-to-apical transport of quinacrine was greater than its apical-to-basolateral transport. In the presence of P-glycoprotein (P-gp) inhibitor, cyclosporine or verapamil, the apical-to-basolateral transport of quinacrine increased. The uptake of quinacrine by MBEC4 cells was enhanced in the presence of cyclosporine or verapamil.

3. Quinacrine uptake was highly concentrative, this event being carried out by a saturable and carrier-mediated system with an apparent K_m of 52.1 μM. Quinacrine uptake was insensitive to Na^+-depletion and changes in the membrane potential and sensitive to changes in pH. This uptake was decreased by tetraethylammonium and cimetidine, a substrate and an inhibitor of organic cation transporters, respectively.

4. These findings suggest that quinacrine transport at the BBB is mediated by the efflux system (P-gp) and the influx system (organic cation transporter-like machinery).

KEY WORDS: quinacrine; blood–brain barrier; mouse brain endothelial cells; P-glycoprotein; organic cation transporter; Creutzfeldt–Jakob disease.

INTRODUCTION

Prion diseases including Creutzfeldt–Jakob disease (CJD) are progressive, fatal neurodegenerative diseases induced by conformational changes in prion protein (PrP) in

[1] Department of Medico-Pharmaceutical Sciences, Graduate School of Pharmaceutical Sciences, Kyushu University, Fukuoka, Japan.
[2] Department of Pharmaceutical Care and Health Sciences, Faculty of Pharmaceutical Sciences, Fukuoka University, Fukuoka, Japan.
[3] Institute of Molecular and Cellular Biosciences, University of Tokyo, Tokyo, Japan.
[4] Nagasaki University Graduate School of Biomedical Sciences, Nagasaki, Japan.
[5] To whom correspondence should be addressed at Department of Pharmaceutical Care and Health Sciences, Faculty of Pharmaceutical Sciences, Fukuoka University, 8-19-1 Nanakuma, Jonan-ku, Fukuoka 814-0180, Japan; e-mail: ykataoka@cis.fukuoka-u.ac.jp.

0272-4340/04/0400-0205/0

the central nervous system. It has been reported that quinacrine, an antimalarial drug, could rapidly eradicate production of the disease-associated and protease-resistant isoform of the prion protein (PrP^{SC}) in vitro (Korth *et al.*, 2001). A clinical trial of quinacrine has started at the Department of Neurology, Faculty of Medicine, Fukuoka University and the Department of Neurology, Faculty of Medicine, Nagasaki University. A transient improvement was observed in CJD patients (Follette, 2003).

The members of organic cation transporter (OCT) family include OCT1 (Grundemann *et al.*, 1994), OCT2 (Okuda *et al.*, 1996), OCT3 (Kekuda *et al.*, 1998), novel organic cation transporter (OCTN)1 (Tamai *et al.*, 1997), OCTN2 (Wu *et al.*, 1998), and OCTN3 (Tamai *et al.*, 2000). The tissue distribution patterns of the OCT family are dependent on the animal species. In the human and rat brain, OCT2 mRNA (Koepsell, 1998), OCTN1 mRNA (Tamai *et al.*, 1997; Wu *et al.*, 2000), and OCTN2 mRNA (Wu *et al.*, 1998, 1999) have been detected. OCTN1 and OCTN2 are expressed in the mouse brain (Tamai *et al.*, 2000). Immortalized rat brain endothelial cells (RBE4) express OCTN2 (Friedrich *et al.*, 2003). OCTN1 and OCTN2 are structurally much more closely related to each other than to OCT1, OCT2, and OCT3 (Wu *et al.*, 2000). Quinacrine is an organic cation and an organic base. The entry of organic cations such as choline into the brain occurs via transport systems present in the blood brain barrier (BBB) (Friedrich *et al.*, 2001; Sawada *et al.*, 1999). The transport of L-carnitine was mediated by OCTN2 in RBE4 cells (Friedrich *et al.*, 2003). Quinacrine inhibited tetraethylammonium (TEA) transport in MDCK cells expressing rat OCT2 (Sweet and Pritchard, 1999).

The BBB permeability of quinacrine is a determinant of its therapeutic efficacy for CJD. Quinacrine is known to pass through the BBB (Korth *et al.*, 2001), although the extent of quinacrine penetration into the brain and the mechanism involved in quinacrine transport across the BBB remain obscure. In this study, we investigated the properties of quinacrine transport into the brain using mouse brain capillary endothelial cells (MBEC4).

MATERIALS AND METHODS

Materials

Quinacrine dihydrochloride and sodium azide (NaN_3) were purchased from Tokyo Kasei Kogyo (Tokyo, Japan) and Kishida Kagaku (Osaka, Japan), respectively. N-Methylglucamine, 2,4-dinitrophenol (DNP), carbonyl cyanide *p*-(trifluoromethoxy) phenylhydrazone (FCCP), valinomycin, amiloride, tetraethylammonium (TEA), cimetidine, and verapamil were purchased from Sigma (St. Louis, MO). Cyclosporine was kindly supplied by Novartis (Basel, Switzerland). All other chemicals were commercial products of reagent grade.

Cell Culture

MBEC4 cells isolated from BALB/c mice brain cortices and immortalized by SV40-transformation (Tatsuta *et al.*, 1992) were cultured in Dulbecco's modified Eagle's medium (DMEM) (GIBCO BRL, Life Technologies, Grand Island, NY)

supplemented with 10% fetal bovine serum, 100 units/mL penicillin, and 100 μg/mL streptomycin in a humidified atmosphere of 5% CO_2/95% air at 37°C. For the transport experiments, MBEC4 cells (42,000 cells/cm^2) were plated into the collagen-coated polycarbonate membrane (1.0 cm^2, 3.0-μm pore size) of the Transwell™ insert (12-well type) (Costar, MA). For the cellular uptake experiments, cells were seeded at a density of 21,000 cells/cm^2 on 4- or 24-well multi dishes (Nunc, Roskilde, Denmark). MBEC4 cells were cultured for 3 days and then used for the following experiments. MBEC4 cells show both general brain endothelial and specific BBB characteristics including the expression of P-glycoprotein (P-gp) (Tatsuta *et al.*, 1992, 1994).

Transcellular Transport of Quinacrine Across MBEC4 Cells

To initiate the transport experiments, the medium was removed and cells were washed three times with Krebs-Ringer buffer (118 mM NaCl, 4.7 mM KCl, 1.3 mM $CaCl_2$, 1.2 mM $MgSO_4$, 1.0 mM NaH_2PO_4, 25 mM $NaHCO_3$, 11 mM D-glucose, pH 7.4). Krebs-Ringer buffer was applied on the outside of the insert in the well (abluminal side) (1.5 mL) and the luminal side of the insert (0.5 mL). Krebs-Ringer buffer containing 50–200 μM quinacrine (MW 473) or 100 μM sodium fluorescein (Na-F) (MW 376), a paracellular transport marker, was loaded on the luminal or abluminal side of the insert. Samples (0.5 mL) were removed from the luminal or abluminal chamber at 10, 20, 30, and 60 min and immediately replaced with fresh Krebs-Ringer buffer. The quinacrine concentration in the samples was determined using a multiwell fluorometer (Ex(λ) 450 nm; Em(λ) 530 nm) (CytoFluor Series 4000, PerSeptive Biosystems, Framingham, MA). Aliquots (5 μL) from the samples were mixed with 200 μL of Krebs-Ringer buffer and then the concentration of Na-F was measured (Ex(λ) 485 nm; Em(λ) 530 nm). Permeability coefficient and clearance were calculated according to the method described by Dehouck *et al.* (1992). Clearance was expressed as μL of tracer diffusing from the luminal to the abluminal chambers and was calculated from the initial concentration of tracer in the luminal chamber and the final concentration of tracer in the abluminal chamber: *Clearance* (μL) = $[C]_A \times V_A/[C]_L$ where $[C]_L$ is the initial luminal tracer concentration, $[C]_A$ is the abluminal tracer concentration, and V_A is the volume of the abluminal chamber. During the 60-min period of the experiment, the clearance volume increased linearly with time. The average volume cleared was plotted versus time, and the slope was estimated by linear regression analysis. The slope of clearance curves for the MBEC4 monolayer was denoted PS_{app}, where PS is the permeability × surface area product (in μL per min). The slope of the clearance curve with the control membrane was denoted $PS_{membrane}$. The real PS value for the MBEC4 monolayer (PS_{trans}) was calculated from $1/PS_{app} = 1/PS_{membrane} + 1/PS_{trans}$. The PS_{trans} values were divided by the surface area of the Transwell™ inserts to generate the permeability coefficient (P_{trans}, in cm per min).

Cellular Uptake of Quinacrine by MBEC4 Cells

For the uptake experiments, MBEC4 cells were washed three times with uptake buffer (143 mM NaCl, 4.7 mM KCl, 1.3 mM $CaCl_2$, 1.2 mM $MgSO_4$, 11 mM D-glucose,

10 mM HEPES, pH 7.4) and incubated with 0.5 mL of the uptake buffer containing quinacrine (1–200 μM) at 37°C for 1–120 min. After incubation, the buffer was removed and cells were washed three times with ice-cold phosphate-buffered saline. The cells were solubilized with 250 μL of 1 N NaOH. Aliquots of the cell solution were removed for protein assay according to the method of Bradford using a Bio-Rad protein assay kit (Bio-Rad Laboratories, Hercules, CA) (Bradford, 1976). Aliquots (200 μL) of the cell solution were neutralized with 200 μL of 1 N HCl and then sample fluorescence was measured (Ex(λ) 450 nm; Em(λ) 530 nm). Quinacrine uptake is expressed as the cell-to-medium ratio (quinacrine amounts in the cells/quinacrine concentration in the medium).

Estimation of Kinetic Parameters

The kinetic parameters for quinacrine uptake by MBEC4 cells were calculated by fitting the uptake rate (V) to the following equation: $V = (V_{max} \times S)/(K_m + S) + P_{dif} \times S$ where V_{max} is the maximum uptake rate of quinacrine (nmol/15 min/mg protein), S is the quinacrine concentration in the medium (μM), K_m is the Michaelis–Menten constant (μM), P_{dif} is the first-order constant for the nonsaturable component (μL/15 min/mg protein). Curve fitting was performed by the nonlinear least-squares regression program, MULTI (Yamaoka *et al.*, 1981).

Detection of OCTN1 mRNA

Total RNA from MBEC4 cells was extracted using TRIZOL™ reagent (Invitrogen, Carlsbad, CA). The primer pair used in the reverse transcription-polymerase chain reaction (RT-PCR) was designed based on the nucleotide sequence of the mouse OCTN1 transporter. The upper primer was 5′-CCTGTTCTGTGTTCCCC-TGT-3′ and the lower primer was 5′-GGTTATGGTGGCAATGTTCC-3′. The expected size of the RT-PCR product, predicted from the positions of the primers, was 232 bp. A SuperScript One-Step RT-PCR system (Invitrogen) was used for reverse transcription of RNA, and OCTN1 cDNA were amplified by PCR. Amplification was performed in a DNA thermal cycler (PC707; ASTEC, Fukuoka, Japan) according to the following protocol: cDNA synthesis for 30 min at 50°C, predenaturation for 2 min at 94°C; 40 cycles of denaturation for 30 s at 94°C, primer annealing for 30 s at 57°C, and polymerization for 30 s at 70°C; and final extension for 5 min at 72°C. Each 10 μL of PCR product was analyzed by electrophoresis on a 3% agarose (Sigma) gel with ethidium bromide staining. The gels were photographed under UV light using a DC290 Zoom digital camera (Kodak, Rochester, New York).

Statistical Analysis

The results are expressed as means ± SEM. Statistical analysis was performed using the Student's unpaired t test. The differences between means were considered to be significant when P values were less than 0.05.

RESULTS

The MBEC4 permeability coefficient of quinacrine dose-dependently increased from $0.58 \pm 0.025 \times 10^{-3}$ to $2.1 \pm 0.15 \times 10^{-3}$ cm/min, when the quinacrine concentration was increased from 50 to 200 μM. The MBEC4 permeability coefficient of quinacrine (100 μM) was significantly lower than that of Na-F (Fig. 1(A)). Permeability coefficients of the basolateral-to-apical transport of quinacrine and Na-F were $1.1 \pm 0.054 \times 10^{-3}$ and $1.5 \pm 0.17 \times 10^{-3}$ cm/min, respectively, while those of the apical-to-basolateral transport were $0.66 \pm 0.023 \times 10^{-3}$ and $1.5 \pm 0.25 \times 10^{-3}$ cm/min, respectively. The basolateral-to-apical transport of quinacrine was significantly higher than that in the opposite direction of transport (Fig. 1(B)). Cyclosporine (10 μM) and verapamil (20 μM) significantly increased the permeability coefficients of the apical-to-basolateral transport of quinacrine from $0.66 \pm 0.023 \times 10^{-3}$ to $1.15 \pm 0.056 \times 10^{-3}$ cm/min and from $0.57 \pm 0.034 \times 10^{-3}$ to $1.02 \pm 0.080 \times 10^{-3}$ cm/min, respectively (Fig. 1(C)).

Quinacrine uptake by MBEC4 cells was time-dependent and reached to the peak at 30 min after the exposure. The cell-to-medium ratio of quinacrine uptake was $2.37 \pm 0.18 \times 10^3$ μL/mg protein at 1 min after the exposure (Fig. 2(A)). Taking the finding that the cell volume of MBEC4 cells is approximately 3 μL/mg protein (Sawada *et al.*, 1999) into consideration, quinacrine is found to be extensively concentrated in MBEC4 cells. To determine whether this apparent concentrative uptake occurs due to only passive entry followed by intracellular binding, MBEC4 cells were treated with 0.015% Triton X for 10 min (Chan *et al.*, 1998). This treatment significantly reduced quinacrine uptake by 30–40% in the period between 30 and 60 min after the addition of quinacrine (Fig. 2(B)). These findings demonstrated that the apparent concentrative accumulation of quinacrine is not due only to passive entry followed by intracellular binding, because quinacrine, when actively accumulated in MBEC4 cells against a concentration gradient and unbound to the binding sites, leaks from cells into the external media through the permeabilized plasma membrane. The initial rate of quinacrine uptake by MBEC4 cells became saturated at 15-min after the exposure to quinacrine (1–200 μM) (Fig. 2(C)). Analysis of these data indicated the involvement of two transport processes (saturable carrier-mediated and nonsaturable system) in quinacrine uptake by MBEC4 cells. The parameters obtained by kinetic analysis were as follows; $V_{max} = 218 \pm 5.4$ nmol/15 min/mg protein, $K_m = 52.1 \pm 1.7$ μM, and passive permeability constant (P_{dif}) $= 94.3 \pm 1.7$ μL/15 min/mg protein.

Quinacrine uptake during a 15-min period was decreased by preincubation of the cells for 10 min with the metabolic inhibitors, NaN_3 (10 mM), DNP (1 mM), and FCCP (10 μM) (Table I). When the experiment was performed at 4°C, quinacrine uptake was reduced (Table I). This uptake was not affected by replacement of the external sodium with N-methylglucamine (Table I) or by changing the external potassium concentration (4.32 ± 0.09, 4.36 ± 0.19, and $4.62 \pm 0.25 \times 10^3$ μL/mg protein at 0, 4.7, and 100 mM of K^+, respectively) (Fig. 3(A)). Pretreatment of MBEC4 cells for a 10-min period with 10 μM of valinomycin, a K^+ ionophore, did not affect quinacrine uptake (Table I). This uptake was elevated from 1.54 ± 0.04 to $4.56 \pm 0.14 \times 10^3$ μL/mg protein by elevating the external pH from 6.4 to 8.4

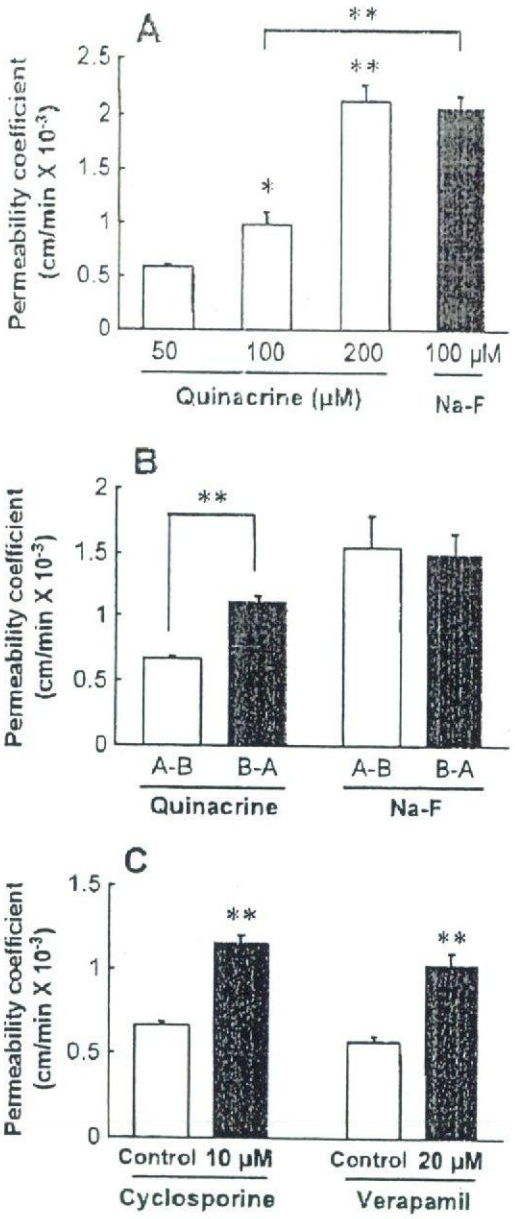

Fig. 1. Characteristics of quinacrine permeability through the MBEC4 monolayer. Panel (A), the permeability coefficients of quinacrine (50–200 μM) or Na-F (100 μM) through the MBEC4 monolayer. Panel (B), the permeability coefficients for the apical-to-basolateral ((A)–(B)) and basolateral-to-apical ((B)–(A)) transport of 100 μM quinacrine and 100 μM Na-F across the MBEC4 monolayer. (A)–(B) and (B)–(A) represent the blood-to-brain and brain-to-blood flux, respectively. Panel (C), the effects of 10 μM cyclosporine and 20 μM verapamil on the apical-to-basolateral transport of 100 μM quinacrine through the MBEC4 monolayer. The permeability coefficient of quinacrine was measured in the presence or absence of each drug. Values are means ± SEM. (n = 3–4 (A), 8 ((B), (C))). * $P < 0.05$ and ** $P < 0.01$; significant difference from the MBEC4 monolayer treated with 50μM quinacrine (A), the opposite direction (B), and the corresponding control (C).

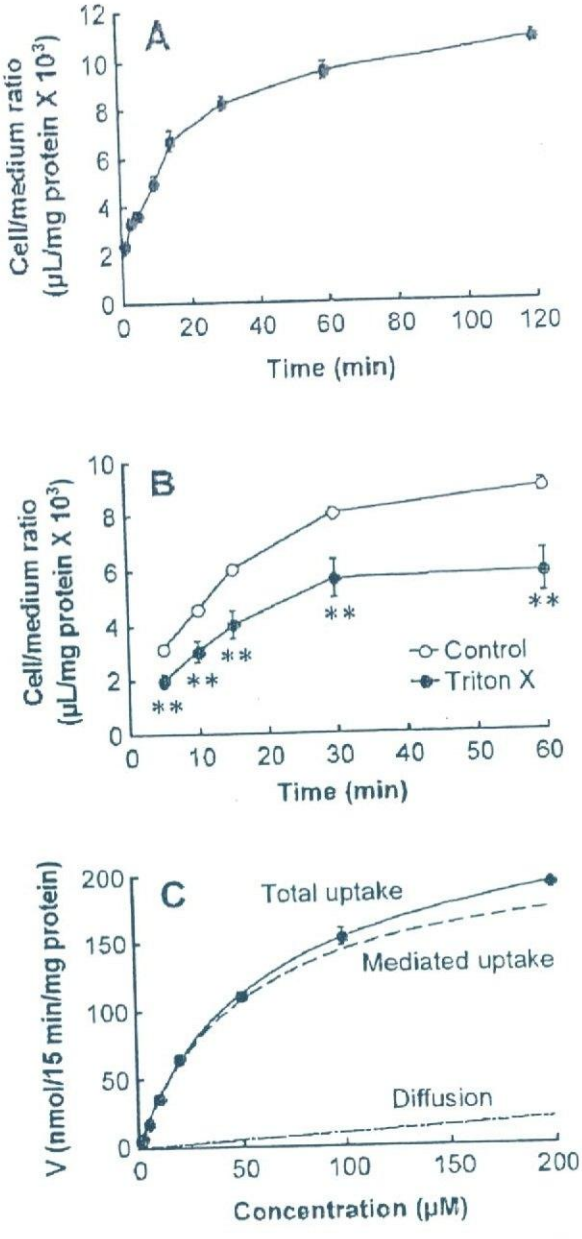

Fig. 2. Characteristics of quinacrine uptake by MBEC4 cells. Panel (A), time course of quinacrine (1 μM) uptake by MBEC4 cells. Panel (B), changes in the quinacrine (1 μM) uptake by MBEC4 cells exposed to 0.015% Triton X for 10 min before the uptake experiment. Panel (C), concentration-dependence of quinacrine uptake by MBEC4 cells. Initial uptake rates at various concentrations of quinacrine (1–200 μM) were measured at 37°C for 15 min. Curves for total, mediated, and diffusive uptake were drawn using the parameters obtained from nonlinear regression analysis (MULTI). Each point represents the mean ± SEM. ($n = 4$–20).** $P < 0.01$; significant difference from the control.

Table I. Effects of Various Compounds and Sodium-Replacement on Uptake of Quinacrine (1 μM) by MBEC4 Cells

Condition	Concentration	Cell/medium ratio (% of control)
NaN_3	10 mM	$67.2 \pm 3.03^{a,**}$
DNP	1 mM	$70.2 \pm 1.79^{a,**}$
4°C		$18.6 \pm 2.22^{a,**}$
FCCP	10 μM	$77.4 \pm 2.49^{a,**}$
Valinomycin	10 μM	97.2 ± 4.22^{a}
Amiloride	1 mM	97.4 ± 3.16^{a}
Tetraethylammonium	1 mM	$88.0 \pm 2.95^{b,**}$
	5 mM	$84.3 \pm 2.93^{b,**}$
	10 mM	$75.4 \pm 4.15^{b,**}$
Cimetidine	1 mM	$81.3 \pm 5.56^{c,**}$
	5 mM	$57.8 \pm 1.70^{c,**}$
	10 mM	$36.8 \pm 1.61^{c,**}$
Na^+ replacement with N-methylglucamine		104 ± 2.87^{d}

[a]MBEC4 cells were preincubated with NaN_3, DNP, FCCP, valinomycin, or amiloride for 10 min. Control values were $4.9 \pm 0.42 \times 10^3$ μL/mg protein. [b,c]Quinacrine uptake was measured by incubating MBEC4 cells with TEA or cimetidine. Control values were 4.1 ± 0.19 and $5.2 \pm 0.19 \times 10^3$ μL/mg protein, respectively.

[d]For investigation of the sodium dependency, quinacrine uptake was measured where Na^+ in the uptake buffer was replaced by N-methylglucamine. Control values were $3.6 \pm 0.22 \times 10^3$ μL/mg protein. Quinacrine uptake was measured at 37°C for 15 min. Values are expressed as % of control. Values are shown as means ± SEM ($n = 4-20$).

** $P < 0.01$; significant difference from the control.

(Fig. 3(B)). These findings demonstrated that quinacrine uptake by MBEC4 cells was pH-dependent. Pretreatment with 10 mM of NaN_3 inhibited quinacrine uptake at each pH used (Table II). Quinacrine uptake was not affected by 1 mM of amiloride (Table I). Therefore, quinacrine uptake was found to be unaffected by Na^+/H^+

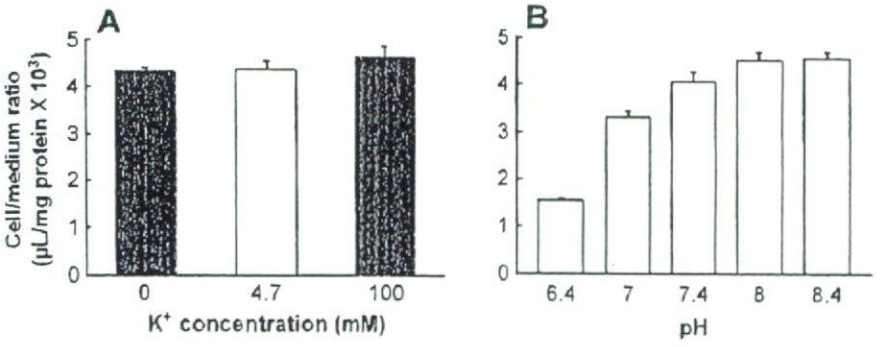

Fig. 3. Effects of the membrane potential (A) and pH (B) on the uptake of quinacrine (1 μM) by MBEC4 cells. Panel (A), effects of various concentrations of external potassium on quinacrine uptake: 0 mM (hyperpolarized), 4.7 mM (control), or 100 mM (depolarized). Panel (B), effects of various pH of the medium on quinacrine uptake. Quinacrine uptake was measured at 37°C for 15 min. Values are expressed as the cell-to-medium ratios. Values are shown as means ± SEM. ($n = 12$).

Table II. Effect of ATP Depletion on the Uptake of Quinacrine (1 μM) by MBEC4 Cells

pH	Cell/medium ratio (μL/mg protein $\times 10^3$)	
	Normal	ATP-depletion
6.4	1.61 ± 0.02	1.36 ± 0.03**
7.0	3.53 ± 0.14	3.28 ± 0.10
7.4	3.95 ± 0.32	3.20 ± 0.33*
8.0	4.71 ± 0.35	3.87 ± 0.30
8.4	4.77 ± 0.19	3.82 ± 0.22*

MBEC4 cells were preincubated with 10 mM NaN_3 for 10 min (ATP depletion). Quinacrine uptake was measured at 37°C for 15 min. Values are shown as means ± SEM ($n = 3$–8).
* $P < 0.05$, ** $P < 0.01$; significant difference from the control.

exchange. The effects of organic cations and P-gp inhibitors on quinacrine uptake were investigated. The organic cations including TEA (1-10 mM) and cimetidine (1–10 mM) significantly reduced quinacrine uptake by 12–25% and 19–65%, respectively (Table I). In the presence of cyclosporine (10 μM) or verapamil (20 μM), quinacrine uptake under the steady-state significantly increased by about 10% (Fig. 4).

To provide molecular evidence for the expression of OCTN1 in MBEC4 cells, RT-PCR was carried out (Fig. 5). With a primer pair specific for mouse OCTN1, RT-PCR with mRNA obtained from MBEC4 cells yielded a single product. The size of this product was the same as that expected from the primer positions in mouse OCTN1.

DISCUSSION

The BBB permeability coefficient of quinacrine, a candidate for the treatment of CJD, was much lower than that of Na-F, a BBB-impermeable marker, suggesting that

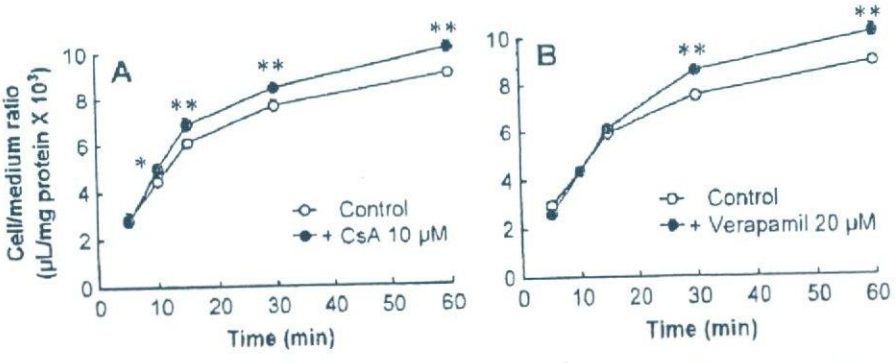

Fig. 4. Effects of 10 μM cyclosporine (A) and 20 μM verapamil (B) on uptake of quinacrine (1 μM) by MBEC4 cells. Quinacrine uptake was measured at 37°C in the absence and presence of cyclosporine or verapamil. Values are expressed as the cell-to-medium ratios. Values are shown as means ± SEM. ($n = 8$).

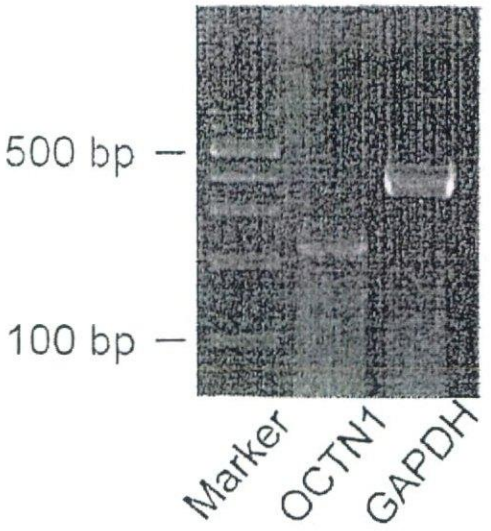

Fig. 5. Photograph showing OCTN1 expression in MBEC4 cells by RT-PCR. RNA samples from MBEC4 cells were used for RT-PCR with primer pairs specific for mouse OCTN1.

the permeability of quinacrine into the brain through the BBB is extremely low. To determine which machinery is involved in the low permeability of quinacrine across the BBB, we investigated the polarity of transcellular transport of quinacrine and the effects of P-gp inhibitors (cyclosporine and verapamil) on the BBB permeability of quinacrine. The basolateral-to-apical (brain-to-blood) transport of quinacrine across MBEC4 monolayer was greater than quinacrine transport in the opposite direction (Fig. 1(B)). Cyclosporine and verapamil increased the apical-to-basolateral (blood-to-brain) transport of quinacrine (Fig. 1(C)). Quinacrine uptake by MBEC4 cells under the steady-state was significantly increased by cyclosporine and verapamil (Fig. 4). These findings indicate the possible involvement of P-gp in the efflux transport of quinacrine. P-gp largely contributes to multidrug-resistance of the BBB in an ATP-dependent manner. This study provided controversial evidence that metabolic inhibitors or incubation at low temperature decreased quinacrine uptake (Table I). Quinacrine was actively and concentratively accumulated in MBEC4 cells. A large part of quinacrine is probably taken up via the saturable system, although quinacrine uptake was shown to have both saturable and nonsaturable pathways (Fig. 2(C)). Uptake of quinacrine by choroid plexus cells was organic cation-specific and energy-dependent (Miller *et al.*, 1999). In light of these findings, P-gp (an efflux system) and other influx transport system(s) are considered to mediate quinacrine transport into the brain.

We elucidated a role of the known organic cation transporters (OCT1, OCT2, OCT3, OCTN1, and OCTN2), and the specificity or driving force of those transporters in mediating quinacrine uptake by MBEC4 cells. Quinacrine uptake was significantly inhibited by various organic cations including TEA and cimetidine, which are known to be a substrate and an inhibitor of the organic cation transporters, respectively. Quinacrine uptake was insensitive to changes in the membrane potential (Fig. 3(A)) and strongly inhibited by lowering the external pH (Fig. 3(B)). These characteristics are distinct from those of the OCT1, OCT2, and OCT3, all of which

are dependent on the membrane potential (Gorboulev *et al.*, 1997; Grundemann *et al.*, 1994; Kekuda *et al.*, 1998). Considering quinacrine is an organic base, the pH-related decrease in quinacrine uptake may have resulted from an increase in the concentration of ionized quinacrine according to the pH partition theory. However, our data showing that quinacrine uptake by MBEC4 cells at each pH was inhibited by NaN_3 (Table II) suggest that a pH-sensitive transport system is involved in quinacrine uptake. Transport of quinacrine increased by elevating the outward H^+ gradient across the membrane. This finding indicates that quinacrine may be transported through MBEC4 cells by an H^+/quinacrine antiport. The activity of H^+/organic cation antiporter is regulated by pH or H^+ gradient as the driving force (Maegawa *et al.*, 1988). The H^+ gradient is formed by Na^+/H^+ exchange in the vicinity of the apical membrane of brain endothelial cells (Ennis *et al.*, 1996). The Na^+/H^+ exchange is, however, unlikely to participate in quinacrine uptake by MBEC4 cells, since Na^+-depletion and amiloride failed to reduce quinacrine uptake (Table I). OCTN1 is Na^+-independent organic cation transporter (Wu *et al.*, 2000). OCTN2 mediates uptake of L-carnitine and several organic cations in an Na^+-coupled and Na^+-independent manner, respectively (Wu *et al.*, 1999). OCTN1 is a pH-dependent organic cation transporter presumably energized by a proton antiport mechanism (Yabuuchi *et al.*, 1999). The characteristics of quinacrine transport obtained in this study are similar to those of OCTN1. Mouse OCTN1 is distributed in the brain, heart, and liver, and strongly expressed in the kidney (Tamai *et al.*, 2000). RT-PCR analysis of MBEC4 cells demonstrated the expression of OCTN1 (Fig. 5). Therefore, OCTN1 is suggested to be a potential transporter mediating quinacrine uptake by MBEC4 cells.

The BBB permeability of quinacrine was extremely low, although quinacrine was rapidly transported into the brain endothelial cells by the apical pH-dependent transport system. A weak organic base binds to a variety of polyanions including RNA, DNA, and ATP, and accumulates in the acidic intracellular compartments (Miller *et al.*, 1999). Quinacrine is distributed in the nucleus and vesicular compartment in the cytoplasm of choroid plexus cells (Miller *et al.*, 1999). In the brain endothelial cells, a large part of quinacrine was shown to be distributed and accumulated in the intracellular binding compartment (Fig. 2(B)). The resulting small part of quinacrine in the intracellular nonbinding compartment appears to contribute to the BBB permeability. The P-gp-mediated active efflux at the apical side of the plasma membrane and the large storage capacity in the cytoplasm are considered to restrict the entry of quinacrine into the brain. The mechanism involved in quinacrine transport at the basolateral side remains obscure.

In conclusion, quinacrine transport at the BBB is mediated by the influx and efflux transport systems. The influx of quinacrine is mediated by a pH-dependent and Na^+- and membrane potential-independent system, an OCTN1-like transporter. The efflux of quinacrine evoked by P-gp at the BBB restricts the entry of quinacrine into the brain. This phenomenon may be interpreted as lowering the therapeutic efficacy of quinacrine for CJD. This study may have clinical implications; quinacrine concentrations in the brain increased by P-gp modulators including verapamil may enhance the therapeutic efficacy of quinacrine for CJD.

ACKNOWLEDGMENTS

This work was supported in part by a Grant-in-Aid for Scientific Research ((B)(2) 14370789) from the Ministry of Education, Culture, Sports, Science, and Technology (MEXT), Japan.

REFERENCES

Bradford, M. M. (1976). A rapid and sensitive method for the quantitation of microgram quantities of protein utilizing the principle of protein dye binding. *Anal. Biochem.* **72**:248–254.

Chan, B. S., Satriano, J. A., Pucci, M., and Schuster, V. L. (1998). Mechanism of prostaglandin E_2 transport across the plasma membrane of HeLa cells and Xenopus oocytes expressing the prostaglandin transporter "PGT". *J. Biol. Chem.* **273**:6689–6697.

Dehouck, M.-P., Jolliet-Riant, P., Brée, F., Fruchart, J.-C., Cecchelli, R., and Tillement, J.-P. (1992). Drug transfer across the blood–brain barrier: Correlation between in vitro and in vivo models. *J. Neurochem.* **58**:1790–1797.

Ennis, S. R., Ren, X., and Betz, A. L. (1996). Mechanisms of sodium transport at the blood-brain barrier studied with in situ perfusion of rat brain *J. Neruochem.* **66**:756–763.

Follette, P. (2003). Prion disease treatment's early promise unravels. *Science* **299**:191–192.

Friedrich, A., George, R. L., Bridges, C. C., Prasad, P. D., and Ganapathy, V. (2001). Transport of cholin and its relationship to the expression of organic cation transporters in a rat brain microvessel cell line (RBE4). *Biochim. Biophys. Acta* **1512**:299–307.

Friedrich, A., Prasad, P. D., Freyer, D., Ganapathy, V., and Brust, P. (2003). Molecular cloning and functional characterization of the OCTN2 transporter at the RBE4 cells, an in vitro model of the blood-brain barrier. *Brain Res.* **968**:69–79.

Gorboulev, V., Ulzheimer, J. C., Akhoundova, A., Ulzheimer-Teuber, I., Karbach, U., Quester, S., Baumann, C., Lang, F., Busch, A. E., and Koepsell, H. (1997). Cloning and characterization of two human polyspecific organic cation transporters. *DNA Cell Biol.* **16**:871–881.

Grundemann, D., Gorboulev, V., Gambaryan, M., Vehyhl, M., and Koepsell, H. (1994). Drug excretion mediated by a new prototype of polyspecific transporter. *Nature* **372**:549–552.

Kekuda, R., Prasad, P. D., Wu, X., Wang, H., Fei, Y. J., Leibach, F. H., and Ganapathy, V. (1998). Cloning and functional characterization of a potential-sensitive, polyspecific organic cation transporter (OCT3) most abundantly expressed in placenta. *J. Biol. Chem.* **273**:15971–15979.

Koepsell, H. (1998). Organic cation transporters in intestine, kidney, liver, and brain. *Annu. Rev. Physiol.* **60**:243–266.

Korth, C., May, B. C. H., Cohen, F. E., and Prusiner, S. B. (2001). Acridine and phenothiazine derivatives as pharmacotherapeutics for prion disease. *Proc. Natl. Acad. Sci. U.S.A.* **98**:9836–9841.

Maegawa, H., Kato, M., Inui, K., and Hori, R. (1988). pH sensitivity of H^+/organic cation antiport system in rat renal brush-border membranes. *J. Biol. Chem.* **263**:11150–11154.

Miller, D. S., Villalobos, A. R., and Pritchard, J. B. (1999). Organic cation transport in rat choroid plexus cells studied by fluorescence microscopy. *Am. J. Physiol.* **276**:C955–C968.

Okuda, N., Saito, H., Urakami, Y., Takano, M., and Inui, K. I. (1996). cDNA cloning and functional expression of a novel rat kidney organic cation transporter. *Biochem. Biophys. Res. Commun.* **224**:500–507.

Sawada, N., Takanaga, H., Matsuo, H., Naito, M., Tsuruo, T., and Sawada, Y. (1999). Choline uptake by mouse brain capillary endothelial cells in culture. *J. Pharm. Pharmacol.* **51**:847–852.

Sweet, D. H., and Pritchard, J. (1999). rOCT2 is a basolateral potential-driven carrier, not an organic cation/proton exchanger. *Am. J. Physiol.* **277**:F890–F898.

Tamai, I., Ohashi, R., Nezu, J., Sai, Y., Kobayashi, D., Oku, A., Shimane, M., and Tsuji, A. (2000). Molecular and functional characterization of organic cation/carnitine transporter family in mice. *J. Biol. Chem.* **275**:40064–40072.

Tamai, I., Yabuuchi, H., Nezu, J., Sai, Y., Oku, A., Shimane, M., and Tsuji, A. (1997). Cloning and characterization of a novel human pH-dependent organic cation transporter, OCTN1. *FEBS Lett.* **419**:107–111.

Tatsuta, T., Naito, M., Mikami, K., and Tsuruo, T. (1994). Enhanced expression by the brain matrix of P-glycoprotein in brain capillary endothelial cells. *Cell Growth Differ.* **5**:1145–1152.

Tatsuta, T., Naito, M., Oh-hara, T., Sugawara, I., and Tsuruo, T. (1992). Functional involvement of P-glycoprotein in blood–brain barrier. *J. Biol. Chem.* **267**:20383–20391.

Wu, X., George, R. L., Huang, W., Wang, H., Conway, S. J., Leibach, F. H., and Ganapathy, V. (2000). Structural and functional characteristics and tissue distribution pattern of rat OCTN1, an organic cation transporter, cloned from placenta. *Biochim. Biophys. Acta* **1466**:315–327.

Wu, X., Huang, W., Prasad, P. D., Seth, P., Rajan, D. P., Leibach, F. H., Chen, J., Conway, S. J., and Ganapathy, V. (1999). Functional characteristics and tissue distribution pattern of organic cation transporter 2 (OCTN2), an organic cation/carnitine transporter. *J. Pharmacol. Exp. Ther.* **290**:1482–1492.

Wu, X., Prasad, P. D., Leibach, F. H., and Ganapathy, V. (1998). cDNA sequence, transport function, and genomic organization of human OCTN2, a new member of the organic cation transporter family. *Biochem. Biophys. Res. Commun.* **246**:589–595.

Yabuuchi, H., Tamai, I., Nezu, J., Sakamoto, K., Oku, A., Shimane, M., Sai, Y., and Tsuji, A. (1999). Novel membrane transporter OCTN1 mediates multispecific, bidirectional, and pH-dependent transport of organic cations. *J. Pharmacol. Exp. Ther.* **289**:768–773.

Yamaoka, K., Tanigawara, Y., Nakagawa, T., and Uno, T. (1981). A pharmacokinetic analysis program (MULTI) for microcomputer. *J. Pharmacobiodyn.* **4**:879–885.

Available online at www.sciencedirect.com

SCIENCE DIRECT

Brain Research 1038 (2005) 208–215

BRAIN RESEARCH

www.elsevier.com/locate/brainres

Research report

Brain pericytes contribute to the induction and up-regulation of blood–brain barrier functions through transforming growth factor-β production

Shinya Dohgu[a], Fuyuko Takata[a], Atsushi Yamauchi[a], Shinsuke Nakagawa[b], Takashi Egawa[a], Mikihiko Naito[c], Takashi Tsuruo[c], Yasufumi Sawada[d], Masami Niwa[b], Yasufumi Kataoka[a,*]

[a]*Department of Pharmaceutical Care and Health Sciences, Faculty of Pharmaceutical Sciences, Fukuoka University, 8-19-1 Nanakuma, Jonan-ku, Fukuoka 814-0180, Japan*

[b]*Department of Pharmacology 1, Graduate School of Medicine, Nagasaki University, 1-12-4 Sakamoto, Nagasaki 852-8523, Japan*

[c]*Institute of Molecular and Cellular Biosciences, University of Tokyo, Bunkyo-ku, Tokyo 113-0032, Japan*

[d]*Department of Medico-Pharmaceutical Sciences, Graduate School of Pharmaceutical Sciences, Kyushu University, 3-1-1 Maidashi, Higashi-ku, Fukuoka 812-8582, Japan*

Accepted 10 January 2005

Abstract

The blood–brain barrier (BBB) is a highly organized multicellular complex consisting of an endothelium, brain pericytes and astrocytes. The present study was aimed at evaluating the role of brain pericytes in the induction and maintenance of BBB functions and involvement of transforming growth factor-β (TGF-β) in the functional properties of pericytes. We used an in vitro BBB model established by coculturing immortalized mouse brain capillary endothelial (MBEC4) cells with a primary culture of rat brain pericytes. The coculture with rat pericytes significantly decreased the permeability to sodium fluorescein and the accumulation of rhodamine 123 in MBEC4 cells, suggesting that brain pericytes induce and up-regulate the BBB functions. Rat brain pericytes expressed TGF-β1 mRNA. The pericyte-induced enhancement of BBB functions was significantly inhibited when cells were treated with anti-TGF-β1 antibody (10 μg/ml) or a TGF-β type I receptor antagonist (SB431542) (10 μM) for 12 h. In MBEC4 monolayers, a 12 h exposure to TGF-β1 (1 ng/ml) significantly facilitated the BBB functions, this facilitation being blocked by SB431542. These findings suggest that brain pericytes contribute to the up-regulation of BBB functions through continuous TGF-β production.

Theme: Cellular and molecular biology
Topic: Blood–brain barrier

Keywords: Blood–brain barrier; Pericyte; Transforming growth factor-β; P-glycoprotein; Permeability; Mouse brain endothelial cell

1. Introduction

The blood–brain barrier (BBB) is highly restrictive of the transport of substances between blood and the central nervous system. The BBB is a complex system of different cellular components including brain microvascular endothelial cells, pericytes and astrocytes. Astrocytes induce and maintain the properties of the BBB including the integration of tight junctions and expression of P-glycoprotein (P-gp) through cell-to-cell contact and the secretion of soluble factors [23]. Brain pericytes are important for control of the growth and migration of endothelial cells and the integrity of microvascular capillaries [22]. Such functions are known to be mediated by transforming growth factor-β (TGF-β) [1,21,25], vascular endothelial growth factor (VEGF)

* Corresponding author. Fax: +81 92 862 2696.
E-mail address: ykataoka@cis.fukuoka-u.ac.jp (Y. Kataoka).

0006-8993/$ - see front matter © 2005 Elsevier B.V. All rights reserved.
doi:10.1016/j.brainres.2005.01.027

[14,17] and direct cell-to-cell communications. Pericytes have several apparatuses to directly make contact with endothelial cells: gap junctions, adhesion plaques and peg-and-socket junctions [24]. Soluble factors including TGF-β, VEGF and basic fibroblast growth factor (bFGF) were produced by and released from pericytes [2,24]. These growth factors control the permeability of the BBB [8,26,31]. These evidences indicate that pericytes regulate the brain's endothelial barrier by collaborating with astrocytes.

TGF-β, a family of multifunctional peptide growth factors, has several isoforms (TGF-β1, 2, 3, 4 and 5), shares the same structure (65–80% homology) and displays similar biological activity in vitro [11]. TGF-β acts on two highly conserved single transmembrane receptors with an intracellular serine/threonine kinase domain (TGF-β type I and type II receptors) to activate an intracellular signaling system, such as Smad proteins or the p38 mitogen-activated protein kinase (MAPK) and the extracellular signal-regulated kinase pathway [6]. TGF-β is listed as a potent endogenous substance protecting against neurodegenerative diseases of the central nervous system [11].

Recently, brain pericytes were reported to induce occludin and multidrug resistance-associated protein (MRP) 6 mRNA expression in brain endothelial cells [3,15]. As for BBB functions, brain pericytes reduce the endothelial permeability of the brain [13]. However, little is known about the mechanism behind the facilitatory role of brain pericytes in the induction and maintenance of BBB functions. The aim of this study was to clarify whether TGF-β participates in the pericyte-induced regulation of BBB functions. We made an in vitro model of the BBB by coculturing immortalized mouse brain capillary endothelial (MBEC4) cells with rat brain pericytes. MBEC4 cells are known to have the highly specialized characteristics of brain microvascular endothelial cells including the expression of P-gp [28,29]. BBB functions were assessed based on the permeability coefficient of sodium fluorescein (Na-F) and the cellular accumulation of rhodamine 123 in MBEC4 cells as the paracellular permeability of brain endothelial cells and the functional activity of P-gp, respectively.

2. Materials and methods

2.1. Animals

Wistar rats aged 2 weeks old were housed in a room at a temperature of 22 ± 2 °C under a 12-h light/dark schedule (lights on at 7:00 h) and given water and food ad libitum. All the procedures involving experimental animals adhered to the law (No. 105) and notification (No.6) of the Japanese Government and were approved by the Laboratory Animal Care and Use Committee of Fukuoka University.

2.2. MBEC4 cell culture

MBEC4 cells, which were isolated from BALB/c mouse brain cortices and immortalized by SV40-transformation [28], were cultured in Dulbecco's modified Eagle's medium (DMEM; Invitrogen, Carlsbad, CA, USA) supplemented with 10% fetal bovine serum (FBS), 100 units/ml penicillin and 100 μg/ml streptomycin at 37 °C with a humidified atmosphere of 5% CO_2/95% air. They were seeded on 12-well Transwell®-Clear inserts (Costar, MA) and 24-well culture plates (BD FALCON™, BD Biosciences, NJ) at a density of 42,000 cells/insert and 21,000 cells/well, respectively.

2.3. Primary culture of rat pericytes

Rat cerebral pericytes were isolated according to the method of Hayashi et al. [13]. Pure cultures of rat cerebral pericytes were obtained by prolonged culture of isolated brain microvessel fragments under selective culture conditions because microvessel fragments contain 23% pericytes [27]. The cerebral cortices from 2-week-old Wistar rats were cleaned of meninges and minced. The homogenate was digested with collagenase CLS2 (1 mg/ml; Worthington, Lakewood, NJ) and DNase I (37.5 μg/ml; Sigma, St. Louis, MO) in DMEM (Sigma) containing 100 units/ml penicillin, 100 μg/ml streptomycin, 50 mg/ml gentamicin and 2 mM glutamine at 37 °C for 1.5 h. Neurons and glial cells were removed by centrifugation in 20% bovine serum albumin (BSA)-DMEM (1000 × *g* for 20 min). The microvessels obtained in the pellet were further digested with collagenase/dispase (1 mg/ml; Roche, Mannheim, Germany) and DNase I (16.7 μg/ml) in DMEM at 37 °C for 1 h. Microvessel endothelial cell clusters were separated by 33% Percoll (Amersham Biosciences, Piscataway, NJ) gradient centrifugation (1000 × *g* for 10 min). The obtained microvessel fragments were washed twice in DMEM (first 1000 × *g* for 8 min, then, 700 × *g* for 5 min) and placed in uncoated culture flasks in DMEM supplemented with 10% FBS, 100 units/ml penicillin and 100 μg/ml streptomycin at 37 °C with a humidified atmosphere of 5% CO_2/95% air. After 14 days in culture, rat pericytes overgrew brain endothelial cells and reached typically 80–90% confluency. The cells were used at passages 2–3.

2.4. Preparation of three in vitro BBB models

The preparation of the in vitro BBB models was previously described [7]. In brief, rat pericytes (40,000 cells/cm^2) were first cultured on the outside of the collagen-coated polyester membrane (1.0 cm^2, 0.4 μm pore size) of a Transwell®-Clear insert (12-well type, Costar) directed upside down in the well. Two days later, MBEC4 cells (42,000 cells/cm^2) were seeded on the inside of the insert placed in the well of a 12-well culture plate (Costar) (the

opposite coculture system). In the other (bottom coculture) system, rat pericytes (20,000 cells/cm^2) were first cultured in the wells of the 12-well culture plate. After 2 days, MBEC4 cells were seeded on the inside of a Transwell®-Clear insert placed in the plate containing layers of rat pericytes. A monolayer system was also made with MBEC4 cells alone (MBEC4 monolayer).

2.5. Paracellular transport of Na-F

To initiate the transport experiments, the medium was removed and MBEC4 cells were washed three times with Krebs–Ringer buffer (118 mM NaCl, 4.7 mM KCl, 1.3 mM $CaCl_2$, 1.2 mM $MgCl_2$, 1.0 mM NaH_2PO_4, 25 mM $NaHCO_3$ and 11 mM D-glucose, pH 7.4). Krebs–Ringer buffer (1.5 ml) was added to the outside of the insert (abluminal side). Krebs–Ringer buffer (0.5 ml) containing 100 μg/ml of Na-F (MW 376) (Sigma) was loaded on the luminal side of the insert. Samples (0.5 ml) were removed from the abluminal chamber at 30, 60, 90 and 120 min and immediately replaced with fresh Krebs–Ringer buffer. Aliquots (5 μl) of the abluminal medium were mixed with 200 μl of Krebs–Ringer buffer and then the concentration of Na-F was determined with a CytoFluor Series 4000 fluorescence multiwell plate reader (PerSeptive Biosystems, Framingham, MA) using a fluorescein filter pair (Ex(λ) 485 ± 10 nm; Em(λ) 530 ± 12.5 nm). The permeability coefficient and clearance were calculated according to the method described by Dehouck et al. [5]. Clearance was expressed as microliters (μl) of tracer diffusing from the luminal to abluminal chamber and was calculated from the initial concentration of tracer in the luminal chamber and final concentration in the abluminal chamber: Clearance (μl) = $[C]_A \times V_A / [C]_L$, where $[C]_L$ is the initial luminal tracer concentration, $[C]_A$ is the abluminal tracer concentration and V_A is the volume of the abluminal chamber. During a 120-min period of the experiment, the clearance volume increased linearly with time. The average volume cleared was plotted versus time, and the slope was estimated by linear regression analysis. The slope of clearance curves for the MBEC4 monolayer or coculture systems was denoted by PS_{app}, where PS is the permeability-surface area product (in μl/min). The slope of the clearance curve with a control membrane was denoted by $PS_{membrane}$. In the rat pericyte opposite coculture system, the control membrane is the rat pericyte-layered membrane. The real PS value for the MBEC4 monolayer and the coculture system (PS_{trans}) was calculated from $1/PS_{app} = 1/PS_{membrane} + 1/PS_{trans}$. The PS_{trans} values were divided by the surface area of the Transwell inserts to generate the permeability coefficient (P_{trans}, in cm/min).

2.6. Functional activity of P-gp

The functional activity of P-gp was determined by measuring the cellular accumulation of rhodamine 123 (Sigma) according to the method of Fontaine et al. [12]. MBEC4 cells were washed three times with assay buffer (143 mM NaCl, 4.7 mM KCl, 1.3 mM $CaCl_2$, 1.2 mM $MgCl_2$, 1.0 mM NaH_2PO_4, 10 mM HEPES and 11 mM D-glucose, pH 7.4). In rat pericyte coculture systems, rat pericytes on the outside of the membrane were removed with a cell scraper. MBEC4 cells were incubated with 0.5 ml of assay buffer containing 5 μM of rhodamine 123 for 60 min. Then, the solution was removed and the cells were washed three times with ice-cold phosphate-buffered saline and solubilized in 1 M NaOH (0.2 ml). Aliquots (5 μl) of the cell solution were removed for measurement of cellular protein according to the method of Bradford [4] using a Bio-Rad protein assay kit (Bio-Rad Laboratories, Hercules, CA). The remaining solution was neutralized with 1 M HCl and the rhodamine 123 content was determined with a CytoFluor Series 4000 fluorescence multiwell plate reader (PerSeptive Biosystems) using a fluorescein filter pair (Ex(λ) 485 ± 10 nm; Em(λ) 530 ± 12.5 nm).

2.7. Detection of TGF-β1 mRNA

Total RNA from rat pericytes was extracted using TRIzol™ reagent (Invitrogen). The primer pair used in the reverse transcription-polymerase chain reaction (RT-PCR) was designed based on the nucleotide sequence of the rat TGF-β1 and rat GAPDH. The sequences of primers were as follows: the upper primer 5′-ATACGCCTGAGTGGCTGTCT-3′ and the lower primer 5′-TGGGACTGATCCCATTGATT-3′ for TGF-β1; the upper primer 5′-CTACCCACGGCAAGTTCAAT-3′ and the lower primer 5′-GGATGCAGGGATGATGTTCT-3′ for GAPDH. The expected sizes of the RT-PCR products, predicted from the positions of the primers, were 153 bp for TGF-β1 and 479 bp for GAPDH. A SuperScript One-Step RT-PCR system (Invitrogen) was used for reverse transcription of RNA, and TGF-β1 cDNA was amplified by PCR. Amplification was performed in a DNA thermal cycler (PC707; ASTEC, Fukuoka, Japan) according to the following protocol: cDNA synthesis for 30 min at 50 °C, pre-denaturation for 5 min at 94 °C; 25 cycles of denaturation for 30 s at 94 °C, primer annealing for 30 s at 57 °C and polymerization for 30 s at 72 °C; and a final extension for 5 min at 72 °C. Each 10 μl of PCR product was analyzed by electrophoresis on a 3% agarose (Sigma) gel with ethidium bromide staining. The gels were visualized on a UV light transilluminator and photographed using a DC290 Zoom digital camera (Kodak, Rochester, New York).

2.8. Effects of the modulation of TGF-β1 signaling on BBB functions

A TGF-β type I receptor antagonist, SB431542 (TOCRIS, Bristol, UK), and human TGF-β1 (Sigma) were first dissolved in dimethylsulfoxide (DMSO) and 4 mM HCl

containing 1 mg/ml BSA, respectively. They were diluted with serum-free culture medium (0.1% as the final DMSO concentration). MBEC4 cells were cultured for 3 days in the three in vitro BBB models. The inserts and wells were washed three times with serum-free medium prior to the experiments. To examine the influence of the inhibition of TGF-β1 signaling on the pericyte-induced changes in BBB functions, SB431542 (10 μM) and monoclonal anti-human TGF-β1 antibody (10 μg/ml; R&D Systems, Minneapolis, MN) were loaded in both compartments of the opposite coculture system. In the MBEC4 monolayer, cells were exposed to 1 ng/ml TGF-β1 injected into the inside (luminal) or outside (abluminal) of the insert for 12 h and subjected to experiments to test whether MBEC4 cells exhibit functional polarity in response to TGF-β1. TGF-β1 and the TGF-β1 receptor antagonist (SB431542) were applied for 12 h to the inside of the insert in the MBEC4 monolayer to investigate the effect of SB431542 on the TGF-β1-induced changes in BBB functions. In all experiments, controls were performed by treating cells with serum-free medium containing the corresponding amount of DMSO and/or 4 mM HCl containing 1 mg/ml BSA as the vehicle.

2.9. Statistical analysis

Values are expressed as the mean ± SEM. Statistical analysis was performed using Student's *t* test. One-way and two-way analyses of variance (ANOVAs) followed by Tukey–Kramer's tests were applied to multiple comparisons. The differences between means were considered to be significant when *P* values were less than 0.05.

3. Results

3.1. BBB functions in three in vitro BBB models and expression of TGF-β1 mRNA in rat pericytes

After MBEC4 cells were cultured for 3 days, the basal permeability and P-gp efflux pump of MBEC4 cells were evaluated in three models of the BBB (Fig. 1). The permeability coefficient of Na-F for MBEC4 cells significantly decreased by 34.8% and 16.0% in the opposite and bottom coculture systems, respectively, when compared to that in the MBEC4 monolayer (Fig. 1A). The accumulation of rhodamine 123 in MBEC4 cells significantly decreased by 17.8 and 7.8% in the opposite and bottom coculture models relative to the MBEC4 monolayer, respectively (Fig. 1B).

To obtain molecular evidence for the expression of TGF-β1 in rat pericytes, RT-PCR was carried out with a primer pair specific for rat TGF-β1 (Fig. 2). RT-PCR with mRNA obtained from rat pericytes yielded a single product. The size of this product was the same as that expected from the primer positions in rat TGF-β1.

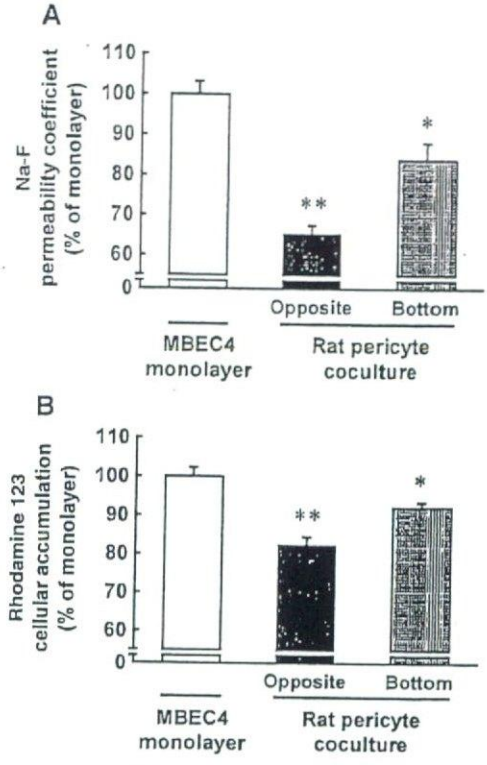

Fig. 1. Permeability and P-gp function of MBEC4 cells in the MBEC4 monolayer and rat pericyte opposite or bottom coculture systems. (A) MBEC4 permeability coefficients of Na-F. Results are expressed relative (%) to the value for the MBEC4 monolayer ($2.7 \pm 0.20 \times 10^{-4}$ cm/min). Values are the means ± SEM (n = 4–12). $^{*}P < 0.05$, $^{**}P < 0.01$, significant difference from MBEC4 monolayer. (B) Rhodamine 123 accumulation in MBEC4 cells. Results are expressed relative (%) to the value for the MBEC4 monolayer (1.61 ± 0.25 nmol/mg protein). Values are the mean ± SEM (n = 4–12). $^{**}P < 0.01$, significant difference from MBEC4 monolayer.

3.2. Effect of the inhibition of TGF-β1 signaling on BBB functions in the MBEC4 monolayer and rat pericyte opposite coculture

As shown in Fig. 3, exposure to anti-TGF-β1 antibody for 12 h inhibited the pericyte-induced enhancement of endothelial barrier and P-gp function in rat pericyte cocultures, whereas anti-TGF-β1 antibody had no significant effect on BBB functions in the MBEC4 monolayer. In the coculture models, anti-TGF-β1 antibody (10 μg/ml) increased the permeability coefficient of Na-F for MBEC4 cells from 86.7 ± 6.1 to 101.7 ± 9.1% of the control value (vehicle-treated MBEC4 monolayer) and the accumulation of rhodamine 123 in MBEC4 cells from 76.6 ± 6.5 to 90.1 ± 8.0% of the control value (Fig. 3). For the permeability to Na-F (Fig. 3A), a two-way ANOVA showed significant effects for the factors culture system (monolayer and coculture) [$F(1, 25) = 4.65$, $P < 0.05$], treatment (vehicle and antibody) [$F(1, 25) = 8.25$, $P < 0.01$] and interaction (culture system × treatment) [$F(1, 25) = 11.51$, $P < 0.005$]. For accumulation of rhodamine 123 (Fig. 3B), a two-way ANOVA showed